

species thus provide unequivocal evidence that the delocalization of the  $\pi$  electrons is responsible for the  $C_{2v}$  cyclic structure, rendering the more metallic heterosystems aromatic. Schaefer and co-workers<sup>[16]</sup> recently performed theoretical studies on model heterocyclic three-membered ring systems related to the  $Ga_3$  organometallic compounds and concluded that these systems were indeed also aromatic.

Herein we extended the concept of aromaticity to the heterocyclic four-membered ring all-metal systems,  $XAl_3^-$ . We showed systematically the importance of the delocalization of the  $\pi$  electrons for the stability of the cyclic aromatic structure. Metallic systems can be aromatic when they are composed of heteroatoms, provided that the heteroatoms have similar electronegativities to the rest of atoms of the ring. However, if the heteroatoms differ substantially in their electronegativities, such as C in  $CAI_3^-$ ,<sup>[14]</sup> the cyclic aromatic structure is no longer a minimum.

Received: January 3, 2001 [Z16366]

- [1] V. I. Minkin, M. N. Glukhovtsev, B. Y. Simkin, *Aromaticity and Antiaromaticity*, Wiley, New York, **1994**.
- [2] G. Raabe, J. Michl in *The Chemistry of Organic Silicon Compounds* (Eds.: S. Patai, Z. Rappoport), Wiley, New York, **1989**, pp. 1102–1108.
- [3] P. v. R. Schleyer, H. Jiao, N. J. R. van Eikema Hommes, V. G. Malkin, O. L. Malkina, *J. Am. Chem. Soc.* **1997**, *119*, 12669.
- [4] X. W. Li, W. T. Pennington, G. H. Robinson, *J. Am. Chem. Soc.* **1995**, *117*, 7578.
- [5] X. W. Li, Y. Xie, P. R. Schreiner, K. D. Gripper, R. C. Crittendon, C. F. Campana, H. F. Schaefer, G. H. Robinson, *Organometallics* **1996**, *15*, 3798.
- [6] G. H. Robinson, *Acc. Chem. Res.* **1999**, *32*, 773.
- [7] X. Li, A. E. Kuznetsov, H. F. Zhang, A. I. Boldyrev, L. S. Wang, *Science* **2001**, *291*, 859.
- [8] A. I. Boldyrev, J. Simons, X. Li, L. S. Wang, *J. Am. Chem. Soc.* **1999**, *121*, 10193.
- [9] L. S. Wang, H. Wu in *Advances in Metal and Semiconductor Clusters*, Vol. 4 (Ed.: M. A. Duncan), JAI Press, Greenwich, **1998**, p. 299.
- [10] X. Li, H. F. Zhang, L. S. Wang, G. D. Geske, A. I. Boldyrev, *Angew. Chem.* **2000**, *112*, 3776; *Angew. Chem. Int. Ed.* **2000**, *39*, 3630.
- [11] L. S. Wang, A. I. Boldyrev, X. Li, J. Simons, *J. Am. Chem. Soc.* **2000**, *122*, 7681.
- [12] We initially optimized the geometries and calculated the frequencies of  $XAl_3^-$  by using analytical gradients with polarized split-valence basis sets (6-311 + G\*) for Al, Si and Ge in  $XAl_3^-$ , and the LANL2DZ basis sets (extending by additional two s, two p and one d functions resulting in (5s5p1d/4s4p1d) basis sets) and the relativistic effective core potentials for Al, Sn, and Pb in  $XAl_3^-$ , and a hybrid method known in the literature as B3LYP. Then we refined the geometries and calculated the frequencies at the second-order Møller-Plesset perturbation theory (MP2) level. The two most stable planar cyclic and pyramidal structures were studied further by using the coupled-cluster method (CCSD(T)) with the same basis sets. The energies of the most stable structures were refined by using the CCSD(T) method, the more extended 6-311 + G(2df) basis sets for Al, Si, and Ge, and (5s5p2d1f/4s4p2d1f) valent basis sets and relativistic core potentials for Al, Sn, and Pb. The vertical electron-detachment energies were calculated by using the outer valence Green Function method (OVGF/6-311 + G(2df) for  $XAl_3^-$  (X = Si, Ge) and OVGF/4s4p2d1f for  $XAl_3^-$  (X = Sn, Pb)), and the CCSD(T)/6-311 + G\* and CCSD(T)/4s4p1d geometries, respectively. All calculations were performed by using the Gaussian 98 program<sup>[13]</sup>.
- [13] Gaussian 98, Revision A.7. M. J. Frisch, G. M. Trucks, H. B. Schlegel, G. E. Scuseria, M. A. Robb, J. R. Cheeseman, V. G. Zakrzewski, J. A. Montgomery, Jr., R. E. Stratmann, J. C. Burant, S. Dapprich, J. M. Millam, A. D. Daniels, K. N. Kudin, M. C. Strain, O. Farkas, J. Tomasi,

- V. Barone, M. Cossi, R. Cammi, B. Mennucci, C. Pomelli, C. Adamo, S. Clifford, J. Ochterski, G. A. Petersson, P. Y. Ayala, Q. Cui, K. Morokuma, D. K. Malick, A. D. Rabuck, K. Raghavachari, J. B. Foresman, J. Cioslowski, J. V. Ortiz, A. G. Baboul, B. B. Stefanov, G. Liu, A. Liashenko, P. Piskorz, I. Komaromi, R. Gomperts, R. L. Martin, D. J. Fox, T. Keith, M. A. Al-Laham, C. Y. Peng, A. Nanayakkara, C. Gonzales, M. Challacombe, P. M. W. Gill, B. G. Johnson, W. Chen, M. W. Wong, J. L. Andres, M. Head-Gordon, E. S. Replogle, J. A. Pople, Gaussian, Inc., Pittsburgh, PA, **1998**.
- [14] A. I. Boldyrev, J. Simons, X. Li, W. Chen, L. S. Wang, *J. Chem. Phys.* **1999**, *110*, 8980.
- [15] The MO pictures were made by using the MOLDEN 3.4 program. G. Schaftenaar, MOLDEN 3.4, CAOS/CAMM Center, The Netherlands, **1998**.
- [16] Y. Xie, P. R. Schreiner, H. F. Schaefer III, X. W. Li, G. H. Robinson, *Organometallics* **1998**, *17*, 114.

## Template-Directed Synthesis of a [2]Rotaxane by the Clipping under Thermodynamic Control of a Crown Ether Like Macrocycle Around a Dialkylammonium Ion\*\*

Peter T. Glink, Ana I. Oliva, J. Fraser Stoddart,\*  
Andrew J. P. White, and David J. Williams\*

New synthetic procedures for preparing rotaxanes<sup>[1]</sup> are appearing in the current literature<sup>[2]</sup> with ever-increasing regularity as a result of the attention<sup>[3]</sup> these mechanically interlocked molecules<sup>[4]</sup> are receiving because of their rapidly growing promise as molecular switches for developing devices<sup>[5]</sup> on the mesoscale and as linear motor-molecules for constructing artificial molecular machinery<sup>[6]</sup> on the nanoscale. One of the simplest recognition motifs that produces pseudorotaxanes,<sup>[7]</sup> complexes that are often the precursors of catenanes and rotaxanes, is the binding<sup>[8]</sup> of dialkylammonium ions with suitably large macrocycles, for example, dibenzo[24]crown-8. Although this motif has so far yielded rotaxanes by both the threading-followed-by-stoppering<sup>[9]</sup> and slippage<sup>[10]</sup> approaches, until now no rotaxanes based on the dialkylammonium ion have been synthesized using a clipping<sup>[11]</sup> protocol. Here, we report the template-directed synthesis<sup>[4c, 12]</sup> of a [2]rotaxane by a clipping approach under thermodynamic control and the subsequent conversion of the dynamic products into a kinetically stable [2]rotaxane which

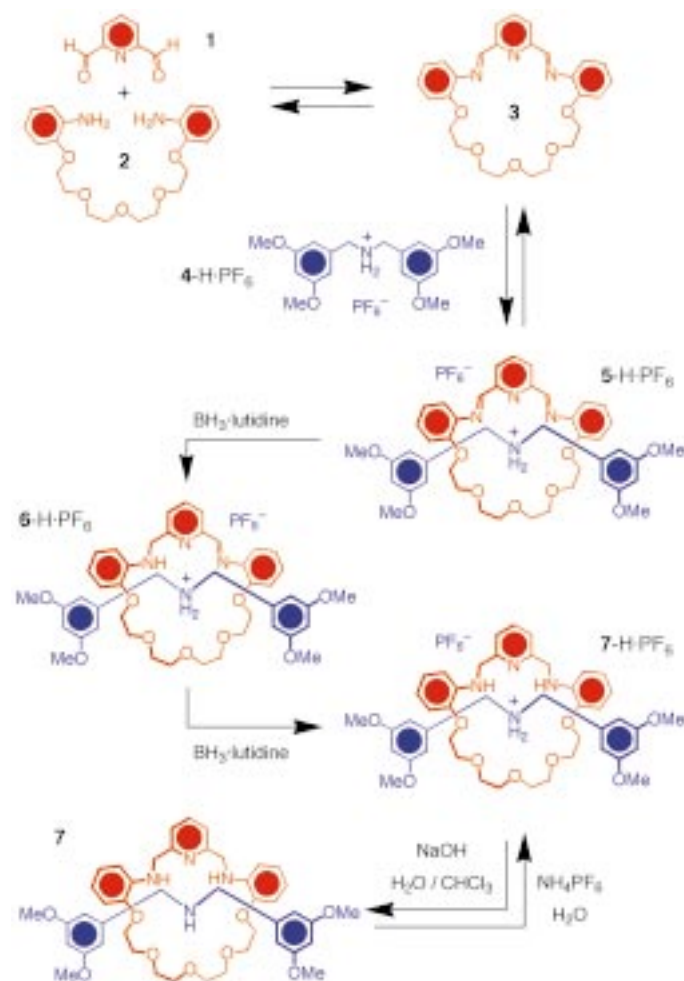
[\*] Prof. J. F. Stoddart, Dr. P. T. Glink, A. I. Oliva  
Department of Chemistry and Biochemistry  
University of California, Los Angeles  
405 Hilgard Avenue, Los Angeles, CA 90095-1569 (USA)  
Fax: (+1) 310-206-1843  
E-mail: stoddart@chem.ucla.edu

Prof. D. J. Williams, Dr. A. J. P. White  
Chemical Crystallography Laboratory, Department of Chemistry,  
Imperial College, South Kensington, London, SW7 2AY (UK)  
Fax: (+44) 207-594-5835

[\*\*] We thank the National Science Foundation for supporting this research, the Spanish Ministry of Education and Sciences (MEC) for a scholarship (A.I.O.), and Sarah K. Hickingbottom and Sheng-Hsien Chiu for donating samples used in this research.

has been isolated and characterized as a neutral as well as a charged compound.

Thermodynamic approaches have become popular methods<sup>[13–16]</sup> of choice for the synthesis of catenanes and rotaxanes. Common dynamic (reversible) reactions exploited in these syntheses include metal–ligand exchanges,<sup>[13]</sup> olefin metatheses,<sup>[14]</sup> opening and closing of disulfide linkages,<sup>[15]</sup> and imine formation<sup>[16]</sup> from mixtures of aldehydes and amines. Imine formation has not yet been reported for the preparation of rotaxanes by the clipping approach even though macrocycles bearing imino groups can possess crown ether like constitutions suitable for binding<sup>[17]</sup> guest molecules and ions. We reasoned (Scheme 1) that the macrocycle with a



Scheme 1. Synthesis of the [2]rotaxane 7-H·PF<sub>6</sub> by the clipping of dialdehyde **1** and diamine **2** around the dialkylammonium ion 4-H<sup>+</sup>, followed by reduction of the imino bonds.

[24]crown-8 constitution formed by the condensation of 2,6-pyridinedicarboxaldehyde<sup>[18]</sup> (**1**) and tetraethyleneglycol bis(2-aminophenyl)ether<sup>[19]</sup> (**2**) would be suitable for encircling the templating NH<sub>2</sub><sup>+</sup> center of a dialkylammonium ion and, provided bulky stoppers terminated the axle-like components, then a rotaxane incorporating a macrocyclic diimine surrounding a dumbbell-shaped template would be the ultimate outcome of the equilibrium-controlled reaction.

An equilibrated, equimolar (20 mM) mixture of **1** and **2** in CD<sub>3</sub>CN gave (after 24 h) a <sup>1</sup>H NMR spectrum (Figure 1 a) in which broad peaks appear that are indicative of an inter-

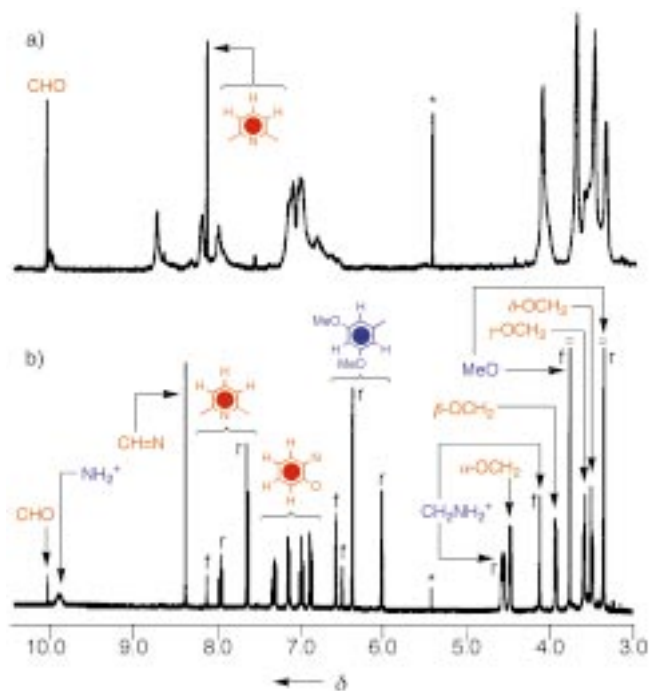


Figure 1. <sup>1</sup>H NMR spectra (360 MHz, CD<sub>3</sub>CN, 298 K) of a) a 1:1 mixture (20 mM) of **1** and **2**, and b) a 1:1:1 mixture (20 mM) of **1**, **2**, and 4-H·PF<sub>6</sub>. The descriptors "r" and "f" refer to signals representing protons in the rotaxane (namely, in 5-H·PF<sub>6</sub>) and in free states, respectively. The signal labeled with an asterisk represents residual CH<sub>2</sub>Cl<sub>2</sub>.

conversion, which is on the order of the NMR timescale at 360 MHz, between imino groups, water, and aldehyde/amino groups. Presumably, the spectrum reflects a mixture of [1+1] (namely, **3**) and higher-order macrocyclic homologues, as well as related acyclic oligomers, all with the potential for displaying *syn/anti* isomerism about their C=N bonds. Addition of bis(3,5-dimethoxybenzyl)ammonium hexafluorophosphate (4-H·PF<sub>6</sub>) has a dramatic effect on the composition of the equilibrium mixture. Equilibrium is established within only 4 min, and sharp resonances appear in the <sup>1</sup>H NMR spectrum (Figure 1 b) for the [2]rotaxane 5-H·PF<sub>6</sub>, in addition to equally sharp resonances for the dumbbell-shaped compound 4-H·PF<sub>6</sub> and broad resonances for the free cyclic and acyclic species that are undergoing exchange with each other on the <sup>1</sup>H NMR timescale. The nature of these resonances suggests that the [2]rotaxane 5-H·PF<sub>6</sub> is thermodynamically stable yet interconverts slowly to its free components on the <sup>1</sup>H NMR timescale at 360 MHz, and that this added stability relative to that of the unthreaded species is a result of [N<sup>+</sup>–H⋯X] (X = O or N) hydrogen bonding and, possibly, also aromatic interactions between the macrocyclic and dumbbell-shaped components of 5-H·PF<sub>6</sub>. Integration of the signals associated with the [2]rotaxane 5-H·PF<sub>6</sub> and those arising from the dumbbell-shaped compound 4-H·PF<sub>6</sub> led to an association constant (*K*<sub>a</sub>) for the formation of 5-H·PF<sub>6</sub> of about 300 L mol<sup>–1</sup> if it is assumed<sup>[20]</sup> that there is an equal

amount of free macrocycle **3** present in the equilibrated mixture. This value of  $K_a$  is comparable with those obtained<sup>[21, 22]</sup> for the associations of dibenzylammonium hexafluorophosphate with either dibenzo[24]crown-8 or *asym*-dibenzo[24]crown-8 in CD<sub>3</sub>CN. FAB mass spectrometric analysis confirmed the stoichiometry of the complex by the presence of a very intense base peak at  $m/z$  793 corresponding to  $[5\text{-H}]^+$ . These observations suggest that **3** displays a similar binding character of the dialkylammonium ion to that exhibited<sup>[21]</sup> by the corresponding dibenzo[24]crown-8 macrocycles, and that the self-assembly<sup>[23]</sup> of  $5\text{-H} \cdot \text{PF}_6$  is a template-directed<sup>[12]</sup> process.<sup>[24]</sup>

The [2]rotaxane  $5\text{-H} \cdot \text{PF}_6$  is kinetically labile as a result of the presence of hydrolyzable imino groups in this compound. These groups can be reduced to the corresponding amino functions to introduce kinetic stability into the rotaxane's structure. We have found that the borane·2,6-lutidine complex<sup>[16b]</sup> is an efficient reducing agent for this process. We monitored the reaction between the equilibrated mixture of the dialdehyde **1**, the diamine **2**, and the dialkylammonium salt  $4\text{-H} \cdot \text{PF}_6$ , in the presence of a slight excess of the  $\text{BH}_3 \cdot \text{lutidine}$  complex in CD<sub>3</sub>CN, and observed (Figure 2) the

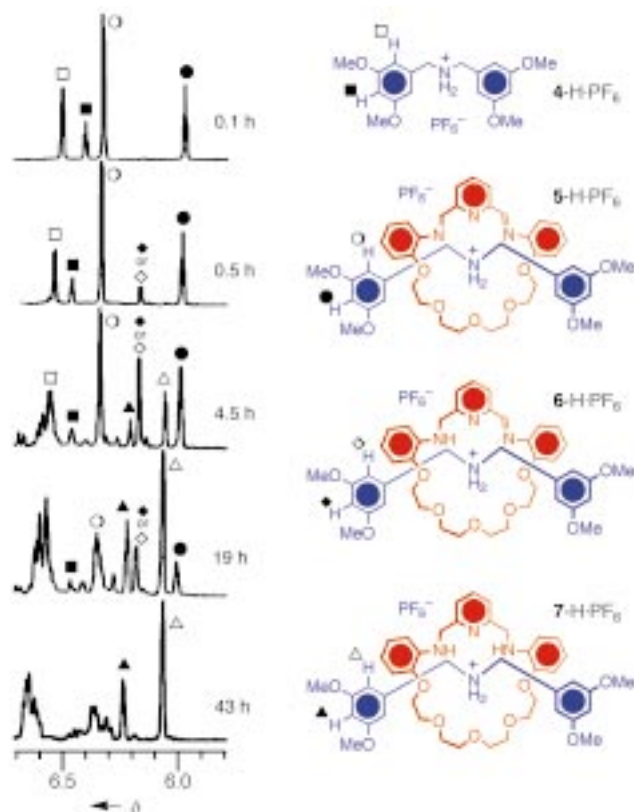


Figure 2. Partial  $^1\text{H}$  NMR spectra (360 MHz, CD<sub>3</sub>CN, 298 K) displaying the signals of the protons on the dimethoxybenzyl units in  $4\text{-H} \cdot \text{PF}_6$  (□/■),  $5\text{-H} \cdot \text{PF}_6$  (○/●),  $6\text{-H} \cdot \text{PF}_6$  (◇/◆), and  $7\text{-H} \cdot \text{PF}_6$  (△/▲) during reduction of the imino groups of  $5\text{-H} \cdot \text{PF}_6$  with  $\text{BH}_3 \cdot 2,6\text{-lutidine}$ .

gradual consumption of  $5\text{-H} \cdot \text{PF}_6$ , the initial appearance and subsequent disappearance of the monoreduced rotaxane  $6\text{-H} \cdot \text{PF}_6$ , and, ultimately, the appearance of the fully reduced rotaxane  $7\text{-H} \cdot \text{PF}_6$ . Interestingly, the signals for the dumbbell-shaped component  $4\text{-H} \cdot \text{PF}_6$  also were observed to disappear

gradually. This observation implies that the reduction of the imino groups in the rotaxanes  $5\text{-H} \cdot \text{PF}_6$  and  $6\text{-H} \cdot \text{PF}_6$  is faster than the corresponding reductions in the free macrocycles (such as **3**) and in linear oligomeric species. The formation of  $7\text{-H} \cdot \text{PF}_6$  results in the equilibrium between the threaded and unthreaded macrocycles producing more  $5\text{-H} \cdot \text{PF}_6$  and  $6\text{-H} \cdot \text{PF}_6$  until, eventually, all of the dialkylammonium salt and macrocyclic precursors are converted into the kinetically stable [2]rotaxane  $7\text{-H} \cdot \text{PF}_6$ . The reason for the faster rate of reduction of the imino groups in the rotaxanes—even though they are much more sterically inaccessible—compared to the unthreaded macrocyclic and acyclic species is believed to reside in the fact that the protonated amino groups in  $5\text{-H} \cdot \text{PF}_6$  and  $6\text{-H} \cdot \text{PF}_6$  provide a weakly acidic environment for the catalysis of the addition of  $\text{BH}$  to imine bonds. Hydrolysis of the B–N bonds formed upon reduction of the imino groups, to yield the aniline-like amino groups, is presumably effected by the water formed by the condensation of **1** and **2**. The free-base [2]rotaxane **7** was isolated in 70 % yield after a workup that included washing with aqueous NaOH and chromatography of the residue on SiO<sub>2</sub> (1 % Et<sub>3</sub>N in MeOH). The X-ray crystal structure<sup>[25, 26]</sup> of **7** reveals (Figure 3) the formation of a [2]rotaxane in which the

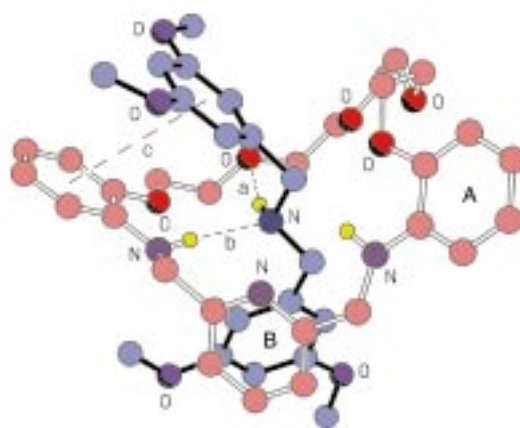


Figure 3. Ball-and-stick representation of the solid-state structure of the neutral [2]rotaxane **7**. Hydrogen-bonding geometries  $[\text{N} \cdots \text{X}]$  [Å],  $[\text{N}-\text{H} \cdots \text{X}]$  [°]: a: 3.24, 2.35, 169 and b: 3.02, 2.13, 169. The centroid  $\cdots$  centroid and mean interplanar separations [Å] are c: 4.01, 3.69; the rings are inclined by about 12°.

dumbbell-shaped component is threaded through the central cavity of the triaza crown ether. The co-conformation is stabilized by  $\text{N}-\text{H} \cdots \text{O}$  and  $\text{N}-\text{H} \cdots \text{N}$  hydrogen bonds between 1) the central amino group of the dumbbell-shaped component and one of the  $\beta$ -ether oxygen atoms of the macrocycle (interaction a) and 2) one of the aminophenol NH groups of the aza crown ether macrocycle and the nitrogen atom of the thread (interaction b). These interactions are supplemented by a  $\pi-\pi$  stacking interaction between one of the 3,5-dimethoxyphenyl rings of the thread and one of the aminophenol rings of the aza crown ether (interaction c). The only inter[2]rotaxane interactions of note are  $\text{C}-\text{H} \cdots \pi$  interactions between centrosymmetrically related pairs of molecules, which involve, in each case, the *ortho* hydrogen

atom of ring A (*syn* to the amino group) in one molecule, and ring B of the thread of the other [ $\text{H} \cdots \pi$  2.79 Å,  $\text{C}-\text{H} \cdots \pi$  148°].

The [2]rotaxane **7** was converted into its hexafluorophosphate salt **7-H**·PF<sub>6</sub> by washing a solution of **7** in CH<sub>2</sub>Cl<sub>2</sub> with saturated aqueous NH<sub>4</sub>PF<sub>6</sub>; this protonation procedure relies on the enhanced basicity of amino groups<sup>[27]</sup> in rotaxane structures relative to those in free amines. The interlocked nature of the components of **7-H**·PF<sub>6</sub> was confirmed by its <sup>1</sup>H NMR spectrum, which displays peaks associated with the dumbbell and wheel-shaped components in a 1:1 ratio, and by its FAB mass spectrum, which displays a very intense base peak at *m/z* 797 corresponding to **[7-H]<sup>+</sup>**. A single-crystal X-ray analysis<sup>[26, 28]</sup> of **7-H**·PF<sub>6</sub> shows (Figure 4) it to have a

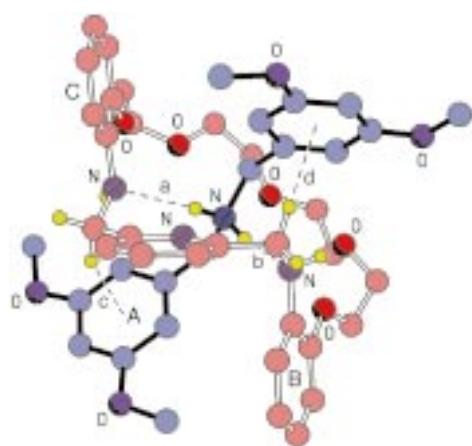


Figure 4. Ball-and-stick representation of the solid-state structure of the cationic [2]rotaxane **7-H<sup>+</sup>**. Hydrogen-bonding geometries [ $\text{N} \cdots \text{N}$ ], [ $\text{H} \cdots \text{N}$ ] [Å], [ $\text{N}-\text{H} \cdots \text{N}$ ] [°]: a: 3.05, 2.18, 163 and b: 3.10, 2.24, 159. The  $\text{H} \cdots \pi$  distances [Å] and  $\text{C}-\text{H} \cdots \pi$  angles [°] are c: 2.82, 144 and d: 2.80, 142.

[2]rotaxane structure that is distinctly different from that of its neutral counterpart **7**. The structure of **7-H**·PF<sub>6</sub> is nearly symmetric, with a molecular C<sub>2</sub> axis passing through the pyridyl nitrogen atom of the triaza crown ether macrocycle and the NH<sub>2</sub><sup>+</sup> center of the cationic thread. The conformations of both the thread and macrocyclic components are distinctly different from those observed for **7**. In **7-H**·PF<sub>6</sub> there are rotations of approximately 39° about both of the pyridyl-CH<sub>2</sub> bonds, with the geometries about the adjacent CH<sub>2</sub>-NH bonds both being *gauche*. These rotations are in contrast to torsional twists in **7** of about 50 and 111° about the pyridyl-CH<sub>2</sub> bonds, and *anti* geometries for their adjacent CH<sub>2</sub>-NH linkages. The torsional twists about the CH<sub>2</sub>-aryl bonds in the cationic dumbbell component are around 70 and 74°, whereas the equivalent twists in the neutral species are about 72 and 36°, respectively. In **7-H**·PF<sub>6</sub> stabilization is achieved by a combination of N<sup>+</sup>-H<sup>+</sup>⋯N and C-H<sup>+</sup>⋯π interactions (a–d in Figure 4). The [2]rotaxanes are loosely linked to their C<sub>i</sub>-related counterparts to form sheets by π–π stacking interactions between rings A and A', B and B', and C and C'; the centroid⋯centroid and mean interplanar separations are 3.95 and 3.52, 4.36 and 3.57, and 4.15 and 3.35 Å, respectively.

The synthesis of the [2]rotaxane **5-H**·PF<sub>6</sub> is an example of a clipping of a macrocycle under thermodynamic control in which the reaction that forms the macrocyclic component appears to be catalyzed by the presence of the dumbbell-shaped component. Moreover, the reduction of the macrocyclic component to yield **7-H**·PF<sub>6</sub> is a good example of template-directed, covalent capture of a self-assembled intermediate under kinetic control.<sup>[29, 30]</sup> This two-step synthesis is reminiscent of enzymatic catalysis<sup>[31]</sup> as well as catalysis<sup>[32]</sup> using synthetic enzyme mimics, inasmuch as there is an initial recognition process—in this instance, the binding of **4-H**·PF<sub>6</sub> with an acyclic form of **3**—that leads to a preorganization of the substrate into a conformation suitable for reaction (in this case, the formation of **5-H**·PF<sub>6</sub>) and a lowering of the activation energy barrier for the final reaction—in this instance, by the acid catalysis resulting from the presence of the NH<sub>2</sub><sup>+</sup> center.

Currently, we are investigating the scope of our new protocol, in addition to extending its application to the template-directed synthesis<sup>[12]</sup> of catenanes and other rotaxanes.

### Experimental Section

A solution of **1** (123 mg, 0.91 mmol), **2** (343 mg, 0.91 mmol), and **4-H**·PF<sub>6</sub> (422 mg, 0.91 mmol) in MeCN was stirred for 5 min at ambient temperature. Evaporation of the solvent yielded a pale-yellow solid. **[5-H**·PF<sub>6</sub>]: <sup>1</sup>H NMR (CD<sub>3</sub>CN, 360 MHz, 298 K): δ = 3.36 (s, 12H), 3.49–3.51 (m, 4H), 3.58–3.61 (m, 4H), 3.92–3.95 (m, 4H), 4.47–4.50 (m, 4H), 4.55–4.60 (m, 4H), 6.05 (t, *J* = 2.2 Hz, 2H), 6.40 (d, *J* = 2.2 Hz, 4H), 6.91 (dd, *J* = 1.6, 7.6 Hz, 2H), 7.02 (dt, *J* = 1.0, 7.6 Hz, 2H), 7.17 (dd, *J* = 1.0, 8.3 Hz, 2H), 7.35 (dt, *J* = 1.6, 8.3 Hz, 2H), 7.67 (d, *J* = 7.8 Hz, 2H), 8.00 (t, *J* = 7.8 Hz, 1H), 8.43 (s, 2H), 9.95 (brs, 2H); MS (FAB): *m/z* (%): 793 (100) **[5-H]<sup>+</sup>**, 476 (10) **[3-H]<sup>+</sup>**. A portion of this solid (100 mg, 0.11 mmol) was dissolved in MeCN and an excess of BH<sub>3</sub>·2,6-lutidine complex (65 mg, 0.54 mmol) was added. The mixture was stirred for 2 days and then the solvent was evaporated. The residue was partitioned between 1M NaOH and CHCl<sub>3</sub> and then the aqueous layer was extracted several times with CHCl<sub>3</sub>. The organic extracts were then dried (MgSO<sub>4</sub>) and the solvent was evaporated. The residue was purified by column chromatography (SiO<sub>2</sub>: MeOH/Et<sub>3</sub>N, 99/1) to yield **7** as a white solid (60 mg, 70%). <sup>1</sup>H NMR (CD<sub>3</sub>CN, 360 MHz, 298 K): δ = 2.70 (brs, 1H), 3.28 (br, 4H), 3.36 (brs, 8H), 3.51 (brs, 4H), 3.55 (s, 12H), 3.99–4.01 (m, 4H), 4.22 (brs, 4H), 6.07 (brt, 2H), 6.19 (brs, 2H), 6.50 (brd, 4H), 6.56 (dt, *J* = 1.6, 7.7 Hz, 2H), 6.68–6.72 (m, 4H), 6.79 (dt, *J* = 1.2, 7.6 Hz, 2H), 7.29 (d, *J* = 7.6 Hz, 2H), 7.43 (t, *J* = 7.6 Hz, 1H); <sup>13</sup>C NMR (CDCl<sub>3</sub>, 90 MHz, 298 K): δ = 50.3, 53.1, 55.1, 67.5, 70.2, 70.6, 70.8, 98.6, 106.5, 109.8, 114.4, 116.1, 122.3, 136.4, 138.3, 146.1, 149.3, 158.1, 160.0; MS (FAB): *m/z* (%): 797 (100) **[7-H]<sup>+</sup>**, 480 (7) **[macrocycle-H]<sup>+</sup>**, 318 (4) **[4-H]<sup>+</sup>**. Single crystals, suitable for X-ray crystallography, of this free-base rotaxane were obtained by liquid diffusion of *i*Pr<sub>2</sub>O into a solution of **7** in CH<sub>2</sub>Cl<sub>2</sub>, followed by slow evaporation. A portion of **7** (30 mg, 38 μmol) was dissolved in CH<sub>2</sub>Cl<sub>2</sub> (1 mL) and washed with saturated NH<sub>4</sub>PF<sub>6</sub> (1 mL). The organic phase was separated, the aqueous phase extracted with CH<sub>2</sub>Cl<sub>2</sub> (3 × 1 mL) and then the combined organic extracts were dried (MgSO<sub>4</sub>) and evaporated to dryness to yield **4-H**·PF<sub>6</sub> as a white solid (34 mg, 95%) <sup>1</sup>H NMR (CDCl<sub>3</sub>, 360 MHz, 298 K): δ = 3.37 (s, 12H), 3.74–3.78 (m, 8H), 3.79–3.80 (m, 4H), 4.00–4.02 (m, 4H), 4.14–4.16 (m, 4H), 4.26 (brs, 2H), 4.50–4.54 (m, 4H), 6.07 (d, *J* = 2.2 Hz, 4H), 6.24 (t, *J* = 2.2 Hz, 2H), 6.36–6.38 (m, 2H), 6.63–6.74 (m, 6H), 7.27 (d, *J* = 7.7 Hz, 2H), 7.76 (t, *J* = 7.7 Hz, 1H), 8.97 (brs, 2H); <sup>13</sup>C NMR (CDCl<sub>3</sub>, 90 MHz, 298 K): δ = 49.6, 53.5, 55.8, 68.5, 71.5, 72.0, 72.3, 101.7, 107.8, 111.3, 113.2, 120.3, 122.3, 124.2, 135.2, 137.9, 147.7, 159.0, 162.0 (1 aryl C missing/overlapping); MS (FAB): *m/z* (%): 797 (100) **[7-H]<sup>+</sup>**. Single crystals, suitable for X-ray crystallography, of this protonated rotaxane were obtained by liquid diffusion of hexane into a solution of **7-H**·PF<sub>6</sub> in Me<sub>2</sub>CO.

Received: January 19, 2001 [Z16457]



- [1] Rotaxanes are molecules comprised of one (or more) wheel-shaped unit(s) that is (are) trapped mechanically along the axle(s) of one (or more) dumbbell-shaped unit(s). See: a) G. Schill, *Catenanes, Rotaxanes and Knots*, Academic Press, New York, **1971**; b) *Molecular Catenanes, Rotaxanes and Knots* (Eds.: J.-P. Sauvage, C. Dietrich-Buchecker), Wiley-VCH, Weinheim, **1999**.
- [2] a) C. Seel, F. Vögtle, *Chem. Eur. J.* **2000**, *6*, 21–24; b) J. E. H. Buston, J. R. Young, H. L. Anderson, *Chem. Commun.* **2000**, 905–906; c) K. Chichak, M. C. Walsh, N. R. Branda, *Chem. Commun.* **2000**, 847–848; d) S. J. Loeb, J. A. Wisner, *Chem. Commun.* **2000**, 1939–1940; e) M.-J. Blanco, J.-C. Chambron, V. Heitz, J.-P. Sauvage, *Org. Lett.* **2000**, *2*, 3051–3054; f) A. J. Baer, D. H. Macartney, *Inorg. Chem.* **2000**, *39*, 1410–1417; g) K.-S. Jeong, J. S. Choi, S.-Y. Chang, H.-Y. Chang, *Angew. Chem.* **2000**, *112*, 1758–1761; *Angew. Chem. Int. Ed.* **2000**, *39*, 1692–1695; h) J. O. Jeppesen, J. Perkins, J. Becher, J. F. Stoddart, *Org. Lett.* **2000**, *2*, 3547–3550.
- [3] a) J.-C. Chambron, J.-P. Sauvage, *Chem. Eur. J.* **1998**, *4*, 1362–1366; b) A. Niemz, V. M. Rotello, *Acc. Chem. Res.* **1999**, *32*, 42–52; c) A. E. Kaifer, *Acc. Chem. Res.* **1999**, *32*, 62–71; d) L. Fabbri, M. Licchelli, P. Pallavicini, *Acc. Chem. Res.* **1999**, *32*, 846–853; e) D. A. Leigh, A. Murphy, *Chem. Ind.* **1999**, 178–183; f) P. Piotrowiak, *Chem. Soc. Rev.* **1999**, *28*, 143–150; g) M.-J. Blanco, M. C. Jiménez, J.-C. Chambron, V. Heitz, M. Linke, J.-P. Sauvage, *Chem. Soc. Rev.* **1999**, *28*, 293–305; h) V. Balzani, A. Credi, M. Venturi, *Supramolecular Science: Where It Is and Where It Is Going* (Eds.: R. Ungaro, E. Dalcanele), Kluwer, Dordrecht, **1999**, pp. 1–22; i) M. D. Ward, *Chem. Ind.* **2000**, 22–26; j) V. Balzani, A. Credi, M. Venturi, in *Stimulating Concepts in Chemistry* (Eds.: M. Shibasaki, J. F. Stoddart, F. Vögtle), Wiley-VCH, Weinheim, **2000**, pp. 255–266.
- [4] a) G. A. Breault, C. A. Hunter, P. C. Mayers, *Tetrahedron* **1999**, *55*, 5265–5293; b) M. B. Nielsen, C. Lombolt, J. Becher, *Chem. Soc. Rev.* **2000**, *29*, 153–164; c) T. J. Hubin, D. H. Busch, *Coord. Chem. Rev.* **2000**, *200–202*, 5–52.
- [5] a) C. P. Collier, E. W. Wong, M. Belohradsky, F. M. Raymo, J. F. Stoddart, P. J. Kuekes, R. S. Williams, J. R. Heath, *Science* **1999**, *285*, 391–394; b) E. W. Wong, C. P. Collier, M. Belohradsky, F. M. Raymo, J. F. Stoddart, J. R. Heath, *J. Am. Chem. Soc.* **2000**, *122*, 5831–5840.
- [6] a) J. A. Preece, J. F. Stoddart, *Nanobiology* **1994**, *3*, 149–166; b) M. Gómez-López, J. A. Preece, J. F. Stoddart, *Nanotechnology* **1996**, *7*, 183–192; c) M. Gómez-López, J. F. Stoddart, *Bull. Soc. Chem. Belg.* **1997**, *106*, 491–500; d) V. Balzani, M. Gómez-López, J. F. Stoddart, *Acc. Chem. Res.* **1998**, *31*, 611–619; e) J.-P. Sauvage, *Acc. Chem. Res.* **1998**, *31*, 611–619; f) V. Balzani, A. Credi, F. M. Raymo, J. F. Stoddart, *Angew. Chem.* **2000**, *112*, 3484–3530; *Angew. Chem. Int. Ed.* **2000**, *39*, 3348–3391.
- [7] Pseudorotaxanes are complexes (supermolecules) that resemble rotaxanes by virtue of being comprised of wheel-like and axle-like components, but their components are free to dissociate from each other. See: P. R. Ashton, D. Philp, N. Spencer, J. F. Stoddart, *J. Chem. Soc. Chem. Commun.* **1991**, 1677–1679.
- [8] a) A. G. Kolchinski, D. H. Busch, N. W. Alcock, *J. Chem. Soc. Chem. Commun.* **1995**, 1289–1291; b) P. T. Glink, C. Schiavo, J. F. Stoddart, D. J. Williams, *Chem. Commun.* **1996**, 1483–1490; c) A. G. Kolchinski, N. W. Alcock, R. A. Roesner, D. H. Busch, *Chem. Commun.* **1998**, 1437–1438; d) M. C. T. Fyfe, J. F. Stoddart, *Adv. Supramol. Chem.* **1999**, *5*, 1–53; e) H. Kawasaki, N. Kihara, T. Takata, *Chem. Lett.* **1999**, 1015–1016; f) W. S. Bryant, I. A. Guzei, A. L. Rheingold, H. W. Gibson, *Org. Lett.* **1999**, *1*, 47–50; g) S. J. Rowan, S. J. Cantrill, J. F. Stoddart, *Org. Lett.* **1999**, *1*, 129–132; h) S. J. Rowan, J. F. Stoddart, *J. Am. Chem. Soc.* **2000**, *122*, 164–165; i) S. J. Cantrill, A. R. Pease, J. F. Stoddart, *J. Chem. Soc. Dalton Trans.* **2000**, 3715–3734.
- [9] The threading-followed-by-stoppering approach to rotaxane assembly relies on the initial formation (by threading) of a pseudorotaxane from wheel- and axle-like components, followed by the attachment (stoppering) of bulky end groups to the axle-like component. For three recent examples involving  $R_2NH_2^+$ -based rotaxanes, see a) J. Cao, M. C. T. Fyfe, J. F. Stoddart, G. R. L. Cousins, P. T. Glink, *J. Org. Chem.* **2000**, *65*, 1937–1946; b) Y. Tachibana, N. Kihara, Y. Ohga, T. Takata, *Chem. Lett.* **2000**, 806–807; c) S. J. Cantrill, D. A. Fulton, A. M. Heiss, A. R. Pease, J. F. Stoddart, A. J. P. White, D. J. Williams, *Chem. Eur. J.* **2000**, *6*, 2274–2287.
- [10] The slippage approach to rotaxane assembly relies on the passage of a wheel-like component over the moderately bulky end groups of a dumbbell-shaped component. For three recent examples involving  $R_2NH_2^+$ -based rotaxanes, see a) P. R. Ashton, M. C. T. Fyfe, C. Schiavo, J. F. Stoddart, A. J. P. White, D. J. Williams, *Tetrahedron Lett.* **1998**, *39*, 5455–5458; b) P. R. Ashton, I. Baxter, M. C. T. Fyfe, F. M. Raymo, N. Spencer, J. F. Stoddart, A. J. P. White, D. J. Williams, *J. Am. Chem. Soc.* **1998**, *120*, 2297–2307; c) S. J. Cantrill, J. A. Preece, J. F. Stoddart, Z.-H. Wang, A. J. P. White, D. J. Williams, *Tetrahedron* **2000**, *56*, 6675–6681.
- [11] The clipping approach to rotaxane assembly relies on the macrocyclization of the subunits of a wheel-like component around the axle-like subunit of the dumbbell-shaped component. For a recent example involving a donor/acceptor-based rotaxane, see ref. [2b].
- [12] a) D. H. Busch, N. A. Stephensen, *Coord. Chem. Rev.* **1990**, *100*, 119–154; b) S. Anderson, H. L. Anderson, J. K. M. Sanders, *Acc. Chem. Res.* **1993**, *26*, 469–475; c) R. Cacciapaglia, L. Mandolini, *Chem. Soc. Rev.* **1993**, *22*, 221–231; d) R. Hoss, F. Vögtle, *Angew. Chem.* **1994**, *106*, 389–398; *Angew. Chem. Int. Ed. Engl.* **1994**, *33*, 375–384; e) *Templated Organic Synthesis* (Eds.: F. Diederich, P. J. Stang), Wiley-VCH, Weinheim, **2000**.
- [13] M. Fujita, *Acc. Chem. Res.* **1999**, *32*, 53–61.
- [14] a) A. C. Try, M. M. Harding, D. G. Hamilton, J. K. M. Sanders, *Chem. Commun.* **1998**, 723–724; b) M. Weck, B. Mohr, J.-P. Sauvage, R. H. Grubbs, *J. Org. Chem.* **1999**, *64*, 5463–5471; c) F. Ibukuro, M. Fujita, Y. Yamaguchi, J.-P. Sauvage, *J. Am. Chem. Soc.* **1999**, *121*, 11014–11015; d) T. J. Kidd, D. A. Leigh, A. J. Wilson, *J. Am. Chem. Soc.* **1999**, *121*, 1599–1600.
- [15] Y. Furusho, T. Hasegawa, A. Tsuboi, N. Kihara, T. Takata, *Chem. Lett.* **2000**, 18–19.
- [16] a) S. J. Cantrill, S. J. Rowan, J. F. Stoddart, *Org. Lett.* **1999**, *1*, 1363–1366; b) S. J. Rowan, J. F. Stoddart, *Org. Lett.* **1999**, *1*, 1913–1916.
- [17] Metal ions are known to bind to these sorts of macrocycles. For a recent example, see L. Valencia, H. Adams, R. Bastida, A. de Blas, D. E. Fenton, A. Macias, A. Rodriguez, T. Rodriguez-Blas, *Inorg. Chim. Acta* **2000**, *300–302*, 234–242.
- [18] U. Luening, R. Baumstark, K. Peters, H.-G. von Schnering, *Liebigs Ann.* **1990**, 129–143.
- [19] H. Sieger, F. Vögtle, *Liebigs Ann.* **1980**, 425–440.
- [20] The calculation of the value of  $K_a$  is only an approximate one since the concentration of **3**, which is participating in other equilibria in the reaction mixture, is unknown. As a result, the calculated value of  $K_a$  is an underestimation of the true value.
- [21] P. R. Ashton, E. J. T. Chrystal, P. T. Glink, S. Menzer, C. Schiavo, N. Spencer, J. F. Stoddart, P. A. Tasker, A. J. P. White, D. J. Williams, *Chem. Eur. J.* **1996**, *2*, 709–728.
- [22] Alkoxy substituents on the *meta* position of the phenyl rings of dibenzylammonium ions have been shown to cause an increase in the values of  $K_a$  relative to those for the unsubstituted dibenzylammonium ion. See: P. R. Ashton, M. C. T. Fyfe, S. K. Hickingbottom, J. F. Stoddart, A. J. P. White, D. J. Williams, *J. Chem. Soc. Perkin Trans. 2* **1998**, 2117–2128.
- [23] a) D. Philp, J. F. Stoddart, *Angew. Chem.* **1996**, *108*, 1242–1286; *Angew. Chem. Int. Ed. Engl.* **1996**, *35*, 1154–1196; b) L. F. Lindoy, I. M. Atkinson, *Self-Assembly in Supramolecular Systems* (Ed.: J. F. Stoddart), Royal Society of Chemistry, Cambridge, **2000**.
- [24] Preliminary results (P. T. Glink, J. Ihringer, J. F. Stoddart) have shown that the nature of the substituents on the phenyl rings of the dibenzylammonium ion affects the association constant for the binding of the salt to macrocycle **3** and plays an important role in determining the rates of both clipping and reduction. We are currently investigating both these thermodynamic and kinetic phenomena.
- [25] Crystal data for **7**:  $C_{45}H_{50}N_4O_9$ ,  $M_r = 796.9$ , triclinic,  $P\bar{1}$  (no. 2),  $a = 9.993(1)$ ,  $b = 13.063(1)$ ,  $c = 16.382(1)$  Å,  $\alpha = 95.90(1)$ ,  $\beta = 90.81(1)$ ,  $\gamma = 92.45(1)^\circ$ ,  $V = 2124.8(2)$  Å<sup>3</sup>,  $Z = 2$ ,  $\rho_{\text{calcd}} = 1.246$  g cm<sup>-3</sup>,  $\mu(\text{Cu}_{K\alpha}) = 7.07$  cm<sup>-1</sup>,  $T = 293$  K, colorless platy needles; 6291 independent measured reflections,  $F^2$  refinement,  $R_1 = 0.048$ ,  $wR_2 = 0.125$ , 5221 independent observed reflections [ $|F_o| > 4\sigma(|F_o|)$ ],  $2\theta \leq 120^\circ$ , 556 parameters.
- [26] Crystallographic data (excluding structure factors) for the structures reported in this paper have been deposited with the Cambridge Crystallographic Data Centre as supplementary publication

- nos. CCDC-156104 (7) and -156105 (7-H · PF<sub>6</sub>). Copies of the data can be obtained free of charge on application to CCDC, 12 Union Road, Cambridge CB2 1EZ, UK (fax: (+44) 1223-336-033; e-mail: deposit@ccdc.cam.ac.uk).
- [27] N. Kihara, Y. Tachibana, H. Kawasaki, T. Takata, *Chem. Lett.* **2000**, 506–507.
- [28] Crystal data for 7-H · PF<sub>6</sub>: [C<sub>45</sub>H<sub>57</sub>N<sub>4</sub>O<sub>9</sub>][PF<sub>6</sub>], *M<sub>r</sub>* = 942.9, triclinic, *P*1̄ (no. 2), *a* = 11.161(1), *b* = 13.517(1), *c* = 16.448(1) Å, *α* = 91.50(1), *β* = 105.53(1), *γ* = 100.67(1)°, *V* = 2342.0(2) Å<sup>3</sup>, *Z* = 2, *ρ*<sub>calcd</sub> = 1.337 g cm<sup>-3</sup>, *μ*(Cu<sub>Kα</sub>) = 12.3 cm<sup>-1</sup>, *T* = 293 K, colorless prisms; 6948 independent measured reflections, *F*<sup>2</sup> refinement, *R*<sub>1</sub> = 0.055, *wR*<sub>2</sub> = 0.142, 5730 independent observed absorption corrected reflections [|*F*<sub>o</sub>| > 4σ(|*F*<sub>o</sub>|)], 2θ ≤ 120°, 624 parameters.
- [29] Previous syntheses of rotaxanes based on dialkylammonium ions under thermodynamic control, either by the threading-followed-by-stoppering (see ref. [9]) or slippage (see ref. [10]) approaches, have not been template-directed ones. Rather, they have afforded products in yields that reflect the association constants of their intermediates.
- [30] For examples of kinetically controlled synthesis of interlocked molecules, see a) D. A. Amabilino, P. R. Ashton, L. Pérez-García, J. F. Stoddart, *Angew. Chem.* **1995**, 107, 2569–2572; *Angew. Chem. Int. Ed. Engl.* **1995**, 34, 2378–2380; b) C. D'Acerno, G. Doddi, G. Ercolani, P. Mencarelli, *Chem. Eur. J.* **2000**, 6, 3540–3546.
- [31] A. J. Kirby, *Angew. Chem.* **1996**, 108, 770–790; *Angew. Chem. Int. Ed. Engl.* **1996**, 35, 707–724.
- [32] For an example of a synthetic receptor with enzyme-like activity, see M. Nakash, Z. Clyde-Watson, N. Feeder, J. E. Davies, S. J. Teat, J. K. M. Sanders, *J. Am. Chem. Soc.* **2000**, 122, 5286–5293.

## Precipitons—Functional Protecting Groups to Facilitate Product Separation: Applications in Isoxazoline Synthesis

Todd Bosanac, Jaemoon Yang, and Craig S. Wilcox\*

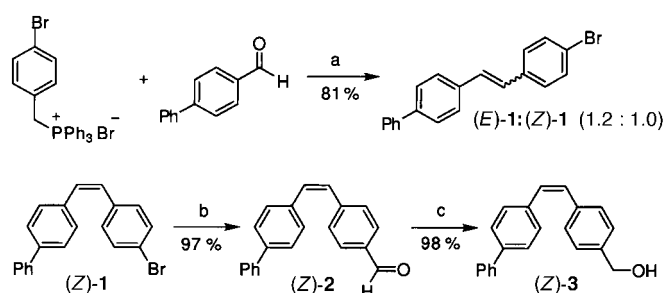
*Dedicated to Prof. Dr. Ronald Breslow  
on the occasion of his 70th birthday symposium*

Automated solid-phase organic synthesis (SPOS) has emerged as an important tool in organic synthesis and medicinal chemistry.<sup>[1]</sup> One of the advantages of SPOS is that the technique allows a large excess of reagents or co-reactants to be employed to ensure that a reaction reaches completion, and these reaction components can then be easily separated from resin-bound products by simple filtration. Although the insoluble nature of the resin is an advantage at the purification stage, it is often a liability at the reaction stage. For example, heterogeneous reaction conditions can complicate monitoring the progress of a reaction by classical methods, and tedious optimization of reaction protocols is sometimes required to obtain good yields in solid-phase reactions. In response to these limitations several research groups have introduced alternatives to SPOS. The new methods (fluorous synthesis,<sup>[2]</sup> soluble polymer-supported organic synthesis

(SPSOS),<sup>[3]</sup> dendrimer-supported organic synthesis,<sup>[4]</sup> and new approaches to acid-base-induced isolation<sup>[5]</sup>) begin with a step in which reactant molecules are attached to “phase-tags”,<sup>[2b]</sup> which are molecular fragments that have special physical properties that facilitate product isolation. These alternatives to solid-phase synthesis share two features: they allow reactions to be carried out under homogeneous conditions, and, after the reaction stage, the product can be isolated by a phase-transfer event (precipitation or liquid–liquid partition) that is induced by the addition of a solvent or by the addition of new co-solutes or reactants.

We envisioned a separation process enabled by a change in solubility that would be caused *not* by a change in solvent or environment, but by structural isomerization of an ancillary portion of the desired product. We define a “precipiton” as a group of atoms (molecular fragment) that is purposefully attached to a reactant molecule and can be isomerized after the reaction to facilitate precipitation or phase transfer of the attached product. One class of precipitons would include molecular fragments that can exist in two isomeric forms: one form freely soluble in a given organic solvent and the other form quite insoluble in that solvent. A product attached to such a molecular fragment could be isolated directly from a reaction mixture by isomerization of the ancillary group to generate the insoluble isomer of the product. The precipitated product would then be isolated by filtration or centrifugation. In the ideal example of this concept of controlled changes in solubility, only products or reagents labeled with the precipiton group would precipitate. Therefore, as in SPOS, excess reagents and co-reactants that might be required to provide good reaction efficiency could be easily removed by filtration.

Our search for such precipitons began with a study of stilbene analogues because *cis*-stilbenes can be more soluble than *trans*-stilbenes.<sup>[6, 7]</sup> The biphenyl-derived alkenes (*Z*)-**3** and (*E*)-**3** were prepared by a Wittig reaction (Scheme 1).



Scheme 1. Synthesis of precipiton (*Z*)-**3**. a) KHMDS, THF, –78 °C, 81%; b) 1. *t*BuLi, THF, –78 °C; 2. DMF, –78 → 0 °C, 97%; c) NaBH<sub>4</sub>, EtOH, 0 °C, 98%. KHMDS = potassium 1,1,1,3,3,3-hexamethyldisilazane.

Alkene (*Z*)-**3** was freely soluble (saturated solutions exceeded 0.2 M) in common organic solvents such as EtOAc, THF, Et<sub>2</sub>O, CH<sub>2</sub>Cl<sub>2</sub>, CHCl<sub>3</sub>, and C<sub>6</sub>H<sub>5</sub>CH<sub>3</sub>. The solubility of (*E*)-**3** in the same solvents were determined by UV/Vis spectroscopic analysis of saturated solutions.<sup>[7, 8]</sup> Isomer (*E*)-**3** was virtually insoluble in all solvents examined (Table 1, entry 1). We prepared dodecyl ether (*E*)-**4** and β-ketoester (*E*)-**5** and measured their solubilities in common organic solvents by the same methods used for (*E*)-**3** (Table 1, entries 2 and 3) to assess the effect that attached productlike groups might have

[\*] Prof. Dr. C. S. Wilcox, T. Bosanac, J. Yang  
Department of Chemistry  
University of Pittsburgh  
Pittsburgh, PA, 15260 (USA)  
Fax: (+1) 412-624-1272  
E-mail: daylite@pitt.edu

Supporting information for this article is available on the WWW under <http://www.angewandte.com> or from the author.